Int J Adv Manuf Technol (2017) 89:3285–3298
DOI 10.1007/s00170-016-9285-x

ORIGINAL ARTICLE

Sculptured surface-oriented machining error synthesis modeling for five-axis machine tool accuracy design optimization

Hai Li[1] · Yingguang Li[1] · Wenping Mou[1] · Xiaozhong Hao[1] · Zhixiang Li[1] · Yan Jin[2]

Received: 3 February 2016 / Accepted: 1 August 2016 / Published online: 18 August 2016

Abstract Customer-oriented design is very important for machine tool manufacturers to win competition in the market. Mechanical parts with complicated sculptured surface are widely utilized in mechanical systems such as automobiles, aircrafts and wind turbines, and they are often machined by five-axis machine tools with high precision requirements. However, traditional machine tool design has not accounted for the varied machining errors in producing complex sculptured surface, which leads to inferior performance. To address this challenge, a novel machining error synthesis model is proposed in this paper for accuracy optimization in designing general five-axis machine tools used for making various sculptured surfaces. The new synthesis model is constructed by integrating a generic machine tool volumetric error model and two new surface machining error production models, and it bridges between the surface machining profile error and the machine tool accuracy. The synthesis model is then applied as a constraint in machine tool accuracy design optimization. A cost-tolerance function is formulated to construct the objective function, and a heuristic algorithm is developed to implement the optimization. These modeling and optimization methods are validated by one case study.

Keywords Accuracy design · Five-axis machine tool · Sculptured surface · Volumetric error · Tolerance design

✉ Yingguang Li
liyingguang@nuaa.edu.cn

[1] College of Mechanical and Electrical Engineering, Nanjing University of Aeronautics and Astronautics, Nanjing, Jiangsu 210016, China

[2] School of Mechanical and Aerospace Engineering, Queen's University Belfast, Belfast, Northern Ireland BT7 1NN, UK

1 Introduction

Customer-oriented design of machine tools is crucial for machine tool manufacturers to gain competiveness in the demanding market. Mechanical parts with complicated sculptured surface are widely utilized in mechanical systems such as automobiles, aircrafts, and wind turbines, and they are often machined by five-axis machine tools with high precision requirements. These requirements are key sources for the customer-oriented design of machine tools.

Machine tool accuracy is one of the most important factors to be taken into account at the machine tool design phase, as the accuracy requirement of a five-axis machine tool affects design decisions which will impact the quality of its individual parts and assemblies. Accuracy parameters of machine tool components are the basic sources to determine the accuracy level of the five-axis machine tool, as specified in the international standards ISO230-6 and ASME B5.54. Also, these desired accuracy parameters restrain or guide the manufacturers' design and construction jobs of a machine tool directly. For example, from the perspective of assembly processes, these parameters are referred to as the assembly tolerances which specify the assembly requirements of the machine tool. Therefore, customer-oriented design is required in determining the design values of these geometrical, dimensional, and tolerance parameters in order to conform to customers' requirements of machining accuracy.

In this paper, an error synthesis model for machining sculptured surface by five-axis machine tools is proposed. This model is established based on two new surface error models and a general machine tool volumetric model. The synthesis model is then applied for design optimization of machine tools. The paper is organized as follows. Section 2 reviews related literature. Accuracy parameters of five-axis machine tools are introduced in Section 3. The new synthesis model is presented in Section 4. In Section 5, a cost-tolerance function is presented, as well as a search heuristic algorithm for machine tool accuracy design optimization. A case study is presented to validate the model and the optimization method via simulations in Section 6. Section 7 concludes the paper.

2 Review of related work

Machining error synthesis is a major method to construct optimization constraints for determining machine tool accuracy parameters. Existing research in this area can be categorized into three classifications, i.e., sensitivity analysis [1, 2], end effector accuracy prediction [1, 3] and error budget [1] of machine tools.

Sensitivity analysis for machine tool errors is the study of how sensitive the output (machining sensitive directional error) of a machine tool can be resulted from different sources of uncertainty in its inputs (machine tool component geometrical errors). Finding the most sensitive errors, which are the main drivers to improve the machining accuracy, is the main focus in this area. Chen [2] carried out the sensitivity analysis of volumetric errors given 37 error components for designing a five-axis ultra-precision machine tool. Li [3] proposed an error modeling method based on multi-solid-body system theory to construct the error mapping between geometrical errors of machine tool components and the cutter's posture error of a five-axis machine tool. The error sensitivity analysis of the five-axis machine tool is then conducted by the error mapping. However, the existing analyses are limited in a plane surface or along the six directions of spatial coordinates; so, these methods are not applicable to the sculptured surfaces because of uncertain sensitive directions.

End effector accuracy prediction, as the name implies, is to predict the output accuracy of a machine tool end effector (such as the spindle or cutter) given the input of machine tool components' errors. Compared to the sensitivity analysis, the end effectors' accuracy prediction results (such as the roundness error of the spindle or the cutter's position and orientation error) are usually used for error compensation. Choi [4] predicted the roundness error of the spindle of a three-axis machine tool through a volumetric error model. Okafor [5] constructed a kinematic model of a three-axis machine tool to predict its cutter's position and orientation error for error compensation, and Rahman [6] constructed a kinematic model of a five-axis machine tool for error measurement. These methods are suitable to calculating the cutter's position and orientation errors, but they are not feasible for estimating the final machining accuracy of the workpiece.

Error budget can be defined as allocating allowable errors to meet a target machining accuracy [1]. Error budget research can be classified into two categories, including the error budget considering the sensitive directions and the error budget considering features and tolerances. Many researchers studied error budget along the sensitive directions. Donaldson [7], Krulewich [8], and Walter [9] conducted the error budget work along the radial direction of lathe machines in order to improve machining accuracy. Kroll [10] analyzed an X-ray inspection machine mainly along its *X*-axis. Erkorkmaz [11] analyzed a precision X-Y working stage along its *X*-, *Y*-, and *Z*-axes, respectively, while Eisenbies [12] analyzed a CMM machine and Sun [13] analyzed an ultraprecision flycutting machine tool along specific directions. Error budget analyses on five-axis machine were also done by Cheng [14], Brecher [15], and Treib [16], and their analyses were also along the *X*-, *Y*-, and *Z*-axes, respectively. Ibaraki [17] identified machine tool errors by machining tests of a stepped workpiece, and a map between the machine tool errors and the workpiece errors is constructed. In summary, all above work is based on the sensitive direction, and they are incapable of dealing with the machining accuracy synthesis of complex workpieces.

Some researchers studied error budget considering features and tolerances [18], because the material removal modeling is also very important for estimating the accurate final parts' shape which is directly linked to customers' requirements. Features are used to describe the shape characteristics of the workpiece, and tolerances are used to describe the allowable variation in shape and position of the features on the workpiece. Nominal tolerance of a feature is just the machining requirement when the machine tool is in machining. For example, a machine error model is proposed to allocate geometric accuracy from the prismatic feature tolerance for machine design [18].

The related research of the above three areas is summarized in Table 1, which accounts for general mechanical machines, precision lathes, three-axis machines, and five-axis machines. Based on the comprehensive review, it is concluded that the design optimization of five-axis machine tool accuracy parameters for machining prismatic features can be realized by existing research [17, 18]. The machining error synthesis model of the machining profile errors of prismatic features (mainly the flatness error) can be naturally built by the error analysis along the normal direction (the sensitive direction) of a flat surface on a prismatic feature. However, the five-axis machine tool errors' effect on the accuracy of machined sculptured surface profiles cannot be established by existing methods, because the complexity of sculptured surface renders the models along sensitive directions invalid. Therefore, the sculptured surface-oriented machining error synthesis modeling is investigated in this paper, and the synthesis model is then used as the constraints in machine tool accuracy design optimization.

3 Accuracy parameters of a five-axis machine tool

From the measurement perspective, these accuracy parameters are mainly quasi-static errors, which contain geometric errors

Table 1 Review of the error synthesis research for machine tools

Application\research field	Sensitivity analysis	End effector accuracy prediction	Error budget considering the sensitive direction	Error budget considering feature and tolerance
Precision lathes	Few academic literatures (For the sensitive direction is obvious, it is easy to determine the sensitive errors in the lathes process).	Few academic literatures.	In Ref. [7–9], lathes machines are analyzed.	Not applicable, for the error budget (without feature and tolerance) along the sensitive direction is enough to address the problem.
Precision three-axis machines	Few academic literatures (For the sensitive direction is obvious, it is easy to determine the sensitive errors in the milling process).	In Ref. [4], roundness error of the spindle of a three axis machine tool is predicted. In Ref. [5], kinematic model is constructed for the prediction, as well as the error compensation.	In Ref. [10], X ray inspection machines by is analyzed. In Ref. [11], a precision X-Y working stage is analyzed. In Ref. [12], a CMM is analyzed. In Ref. [13], a ultraprecision flycutting machine tool is analyzed.	Prismatic feature with tolerance is considered in Ref. [18].
Precision five-axis machines	In Ref. [2], the machining object is the plane surface; In Ref. [3], analyzed target is the six directions of spatial coordinates. They are not applicable for the sculptured surface because of uncertain sensitive directions.	In Ref. [6], kinematic model is constructed for the prediction and error compensation.	In Ref. [14], five-axis machine using laser is analyzed; In Ref. [15], five-axis grinding machine is analyzed. In Ref. [16], five-axis machine tool is analyzed. In Ref. [17], the mapping between the machine tool errors and the stepped workpiece machining errors are constructed.	Few researches about machine tool errors' effect on sculptured surface profile machining error are found, and it is the research goal of this paper.

and thermal errors, as reviewed by Ramesh [19]. From the perspective of tolerance design and assembly process, these accuracy parameters are assembly tolerances which specify the final assembly requirement of machine tool products. In this paper, the quasi-static error components, defined by multi-rigid body kinematics, are used to mathematically express these accuracy parameters. These accuracy parameters will then be the operands of the optimization problem.

3.1 Machine structure

As shown in Fig. 1, a three translational and two rotational DOF (TTTRR) type five-axis machine tool is taken as a general example. Five kinematic pairs including three translational and two rotational axes are defined as the *X*-, *Y*-, *Z*-, *C*- and *A*-axes, respectively. The structure diagram and the kinematic chain diagram are defined complying to the definition in ref. [20].

3.2 Accuracy parameters

The quasi-static errors of machine tools stem from the errors of every individual axis and the errors between axes. The quasi-static error components consist of positioning, straightness, angular, squareness, and parallelism. As a free rigid body has six degrees of freedom, every translational or rotational axis has six quasi-static error components, which contain both linear and angular errors. For a translational axis, the six error components are one linear positioning error, two straightness errors, and three angular errors about pitch, yaw, and roll axes, respectively. For a rotational axis, the three linear error components are one axial error and two radial errors, and the three angular error components are one angular position error and two tilt errors. Also, there exists the squareness errors between *X*- and *Y*-axes, *Y*- and *Z*-axes, *Z*- and *X*-axes and the parallelism error between *A*- and *X*-axes, *C* and *Z*-axes. Therefore, 37 quasi-static errors exist in the five-axis machine tool. These error components are listed in Table 2.

4 Mapping model between machine accuracy parameters and machining accuracy

The profile errors of the surface are caused by the errors in machining. To restrain the machine tool accuracy parameter X_i which are in the form of quasi-static errors, the machine tool quasi-static errors' effect on the machined surface is investigated in this paper. Cutter's posture (include the position and orientation) errors, also known as volumetric errors [2], which

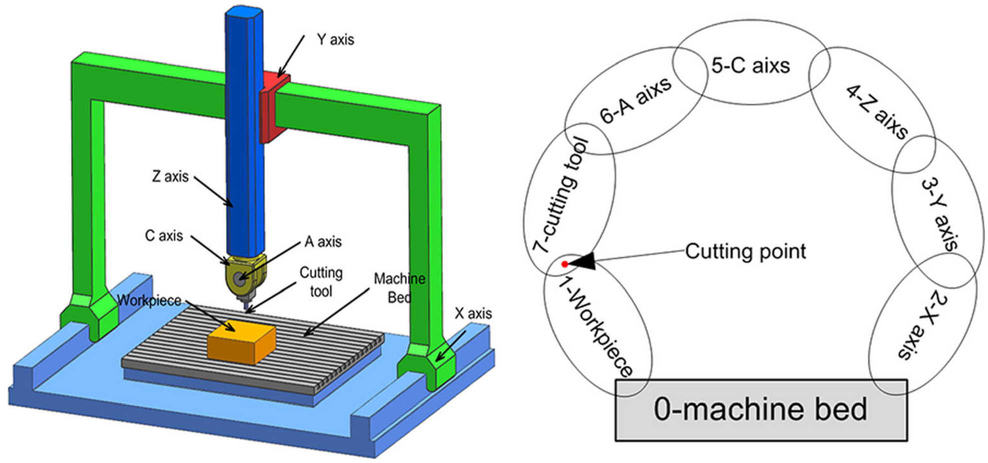

Fig. 1 A TTTRR (XYZCA) type five-axis machine tool and the kinematic chain

are induced by the machine tool errors, will affect the profile errors of the machined surfaces. In other words, the cutter's posture errors are the bridge in between the machine tool errors and the profile errors of the machined surfaces.

4.1 Volumetric error modeling of the machine tool

Volumetric error modeling, which maps between machine tool quasi-static errors and cutter's posture errors, is the first step in finding the relationship between machine tool errors and profile errors of machined surfaces. Rigid body kinematics and homogeneous transform are used for volumetric error modeling in this section. Eight rigid bodies of a general five-axis machine tool shown in Fig. 1 are defined. Two structural chains exist in the machine tool. One is from the bed to the cutter via the machine tool, and the other is from the bed to the workpiece directly. These two chains are called "cutter structural chain" and "workpiece structural chain," respectively. Every rigid body on these two chains is coded by a number. The machine tool bed is usually associated with number 0. Number ***1*** represents the first

Table 2 Expressions of accuracy parameters of five-axis machine tool

Description		Expression	NO.	Description		Expression	NO.
X-axis kinematic pair	Linear	$\varepsilon_x(x)$	1	C axis kinematic pair	Axial	$\varepsilon_x(\gamma)$	19
	Straightness	$\varepsilon_y(x)$	2		Radius	$\varepsilon_y(\gamma)$	20
	Straightness	$\varepsilon_z(x)$	3		Radius	$\varepsilon_z(\gamma)$	21
	Roll	$\varepsilon_\alpha(x)$	4		Tilt	$\varepsilon_\alpha(\gamma)$	22
	Pitch	$\varepsilon_\beta(x)$	5		Tilt	$\varepsilon_\beta(\gamma)$	23
	Yaw	$\varepsilon_\gamma(x)$	6		Angular position	$\varepsilon_\gamma(\gamma)$	24
Y-axis kinematic pair	Linear	$\varepsilon_x(y)$	7	A axis kinematic pair	Axial	$\varepsilon_x(\alpha)$	25
	Straightness	$\varepsilon_y(y)$	8		Radius	$\varepsilon_y(\alpha)$	26
	Straightness	$\varepsilon_z(y)$	9		Radius	$\varepsilon_z(\alpha)$	27
	Pitch	$\varepsilon_\alpha(y)$	10		Angular position	$\varepsilon_\alpha(\alpha)$	28
	Roll	$\varepsilon_\beta(y)$	11		Tilt	$\varepsilon_\beta(\alpha)$	29
	Yaw	$\varepsilon_\gamma(y)$	12		Tilt	$\varepsilon_\gamma(\alpha)$	30
Z-axis kinematic pair	Linear	$\varepsilon_x(z)$	13				
	Straightness	$\varepsilon y(z)$	14				
	Straightness	$\varepsilon_z(z)$	15				
	Yaw	$\varepsilon_\alpha(z)$	16				
	Pitch	$\varepsilon_\beta(z)$	17				
	Roll	$\varepsilon_\gamma(z)$	18				
Between axes	Squareness	$\Delta\gamma_{xy}$	31	Parallelism		$\Delta\beta_{xa}$	34
	Squareness	$\Delta\beta_{zx}$	32	Parallelism		$\Delta\gamma_{xa}$	35
	Squareness	$\Delta\alpha_{yz}$	33	Parallelism		$\Delta\alpha_{zc}$	36
				Parallelism		$\Delta\beta_{zc}$	37

adjacent rigid body in the workpiece structural chain, and the other numbers are assigned as shown in Fig. 1 to represent the rigid bodies in the cutter structural chain. According to the rigid body kinematics in ref. [2, 21], the transformation between the rigid body k and its adjacent rigid body j is described as

$$ {}_{k}^{\mathrm{j}}T^{k} = {}_{k}^{\mathrm{j}}T^{k}{}_{p}\ {}_{k}^{\mathrm{j}}T^{k}{}_{pe}\ {}_{k}^{\mathrm{j}}T^{k}{}_{s}\ {}_{k}^{\mathrm{j}}T^{k}{}_{se}, \tag{1} $$

where ${}_{k}^{\mathrm{j}}T^{k}{}_{p}$, ${}_{k}^{\mathrm{j}}T^{k}{}_{pe}$, ${}_{k}^{\mathrm{j}}T^{k}{}_{s}$, and ${}_{k}^{\mathrm{j}}T^{k}{}_{se}$ are the posture transformation matrix, posture error transformation matrix, motion transformation matrix, and motion error transformation matrix between rigid bodies k and j, respectively. Based on Eq. (1), the transformation matrices between these bodies in the workpiece and cutter structural chain can be obtained as follows.

$$ {}_{2}^{0}T^{2} = \begin{bmatrix} 1 & & & P_{2x} \\ & 1 & & P_{2y} \\ & & 1 & P_{2z} \\ & & & 1 \end{bmatrix} I_{4X4} \begin{bmatrix} 1 & & & x \\ & 1 & & \\ & & 1 & \\ & & & 1 \end{bmatrix} \begin{bmatrix} 1 & -\varepsilon_{\gamma}(x) & \varepsilon_{\beta}(x) & \varepsilon_{x}(x) \\ \varepsilon_{\gamma}(x) & 1 & -\varepsilon_{\alpha}(x) & \varepsilon_{y}(x) \\ -\varepsilon_{\beta}(x) & \varepsilon_{\alpha}(x) & 1 & \varepsilon_{z}(x) \\ & & & 1 \end{bmatrix}, \tag{2} $$

$$ {}_{3}^{2}T^{3} = \begin{bmatrix} 1 & & & P_{3x} \\ & 1 & & P_{3y} \\ & & 1 & P_{3z} \\ & & & 1 \end{bmatrix} \begin{bmatrix} 1 & -\Delta\gamma_{\mathrm{xy}} & & \\ \Delta\gamma_{\mathrm{xy}} & 1 & & \\ & & 1 & \\ & & & 1 \end{bmatrix} \begin{bmatrix} 1 & & & \\ & 1 & & y \\ & & 1 & \\ & & & 1 \end{bmatrix} \begin{bmatrix} 1 & -\varepsilon_{\gamma}(y) & \varepsilon_{\beta}(y) & \varepsilon_{x}(y) \\ \varepsilon_{\gamma}(y) & 1 & -\varepsilon_{\alpha}(y) & \varepsilon_{y}(y) \\ -\varepsilon_{\beta}(y) & \varepsilon_{\alpha}(y) & 1 & \varepsilon_{z}(y) \\ & & & 1 \end{bmatrix}, \tag{3} $$

$$ {}_{4}^{3}T^{4} = \begin{bmatrix} 1 & & & P_{4x} \\ & 1 & & P_{4y} \\ & & 1 & P_{4z} \\ & & & 1 \end{bmatrix} \begin{bmatrix} 1 & & \Delta\beta_{\mathrm{zx}} & \\ & 1 & -\Delta\alpha_{\mathrm{yz}} & \\ -\Delta\beta_{\mathrm{zx}} & \Delta\alpha_{\mathrm{yz}} & 1 & \\ & & & 1 \end{bmatrix} \begin{bmatrix} 1 & & & \\ & 1 & & \\ & & 1 & z \\ & & & 1 \end{bmatrix} \begin{bmatrix} 1 & -\varepsilon_{\gamma}(z) & \varepsilon_{\beta}(z) & \varepsilon_{x}(z) \\ \varepsilon_{\gamma}(z) & 1 & -\varepsilon_{\alpha}(z) & \varepsilon_{y}(z) \\ -\varepsilon_{\beta}(z) & \varepsilon_{\alpha}(z) & 1 & \varepsilon_{z}(z) \\ & & & 1 \end{bmatrix}, \tag{4} $$

$$ {}_{5}^{4}T^{5} = \begin{bmatrix} 1 & & & P_{5x} \\ & 1 & & P_{5y} \\ & & 1 & P_{5z} \\ & & & 1 \end{bmatrix} \begin{bmatrix} 1 & & \Delta\beta_{\mathrm{zc}} & \\ & 1 & -\Delta\alpha_{\mathrm{zc}} & \\ -\Delta\beta_{\mathrm{zc}} & \Delta\alpha_{\mathrm{zc}} & 1 & \\ & & & 1 \end{bmatrix} \begin{bmatrix} \cos\gamma & -\sin\gamma & & \\ \sin\gamma & \cos\gamma & & \\ & & 1 & \\ & & & 1 \end{bmatrix} \begin{bmatrix} 1 & -\varepsilon_{\gamma}(\gamma) & \varepsilon_{\beta}(\gamma) & \varepsilon_{x}(\gamma) \\ \varepsilon_{\beta}(\gamma) & 1 & -\varepsilon_{\alpha}(\gamma) & \varepsilon_{y}(\gamma) \\ -\varepsilon_{y}(\gamma) & \varepsilon_{\alpha}(\gamma) & 1 & \varepsilon_{z}(\gamma) \\ 0 & 0 & 0 & 1 \end{bmatrix}, \tag{5} $$

$$ {}_{6}^{5}T^{6} = \begin{bmatrix} 1 & & & P_{6x} \\ & 1 & & P_{6y} \\ & & 1 & P_{6z} \\ & & & 1 \end{bmatrix} \begin{bmatrix} 1 & -\Delta\gamma_{xa} & & \\ \Delta\gamma_{xa} & 1 & \Delta\beta_{xa} & \\ -\Delta\beta_{xa} & & 1 & \\ & & & 1 \end{bmatrix} \begin{bmatrix} 1 & 0 & 0 & 0 \\ 0 & \cos\alpha & -\sin\alpha & 0 \\ 0 & \sin\alpha & \cos\alpha & 0 \\ 0 & 0 & 0 & 1 \end{bmatrix} \begin{bmatrix} 1 & -\varepsilon_{\gamma}(\alpha) & \varepsilon_{\beta}(\alpha) & \varepsilon_{x}(\alpha) \\ \varepsilon_{\beta}(\alpha) & 1 & -\varepsilon_{\alpha}(\alpha) & \varepsilon_{y}(\alpha) \\ -\varepsilon_{y}(\alpha) & \varepsilon_{\alpha}(\alpha) & 1 & \varepsilon_{z}(\alpha) \\ & & & 1 \end{bmatrix}, \tag{6} $$

$$ {}_{7}^{6}T^{7} = \begin{bmatrix} 1 & & & P_{7x} \\ & 1 & & P_{7y} \\ & & 1 & P_{7z} \\ & & & 1 \end{bmatrix}, \tag{7} $$

$$ {}_{1}^{0}T^{1} = \begin{bmatrix} 1 & & & P_{1x} \\ & 1 & & P_{1y} \\ & & 1 & P_{1z} \\ & & & 1 \end{bmatrix}, \tag{8} $$

where P_{1x}, P_{1y}, and P_{1z} are the position coordinates of the workpiece's coordinate system relative to the bed's coordinate system (as shown in Fig. 2). P_{ix}, P_{iy}, and P_{iz} ($i = 2, 3, 4, 5, 6$) in each transformation are the position coordinates of the ith body relative to the (i-1)th body. P_{7x}, P_{7y}, and P_{7z} are the relative position coordinates between the cutter and the C-axis (the 6th body). x, y, z, α, and γ are the posture parameters associated with the five degrees of freedom of the machine tool. The rest accuracy parameters are shown in Table 2. The workpiece and the cutter are fixed on the bed and the C-axis, respectively, considered as no error, as expressed in Eq. (7) and (8).

R_w and R_t represent the position vectors of the cutting point in the coordinate systems of the workpiece and the cutter, respectively, which are expressed as

$$ R_w = \left[R_{wx}\ \ R_{wy}\ \ R_{wz}\right]^T, \tag{9} $$

and

$$ R_t = [\,R_{tx}\quad R_{ty}\quad R_{tz}\,]T. \tag{10} $$

V_w and V_t represent the orientation vectors of the cutting point in the coordinate systems of the workpiece and the cutter, respectively, which are expressed as

$$ V_w = [\,V_{wx}\quad V_{wy}\quad V_{wz}\,]^T, \tag{11} $$

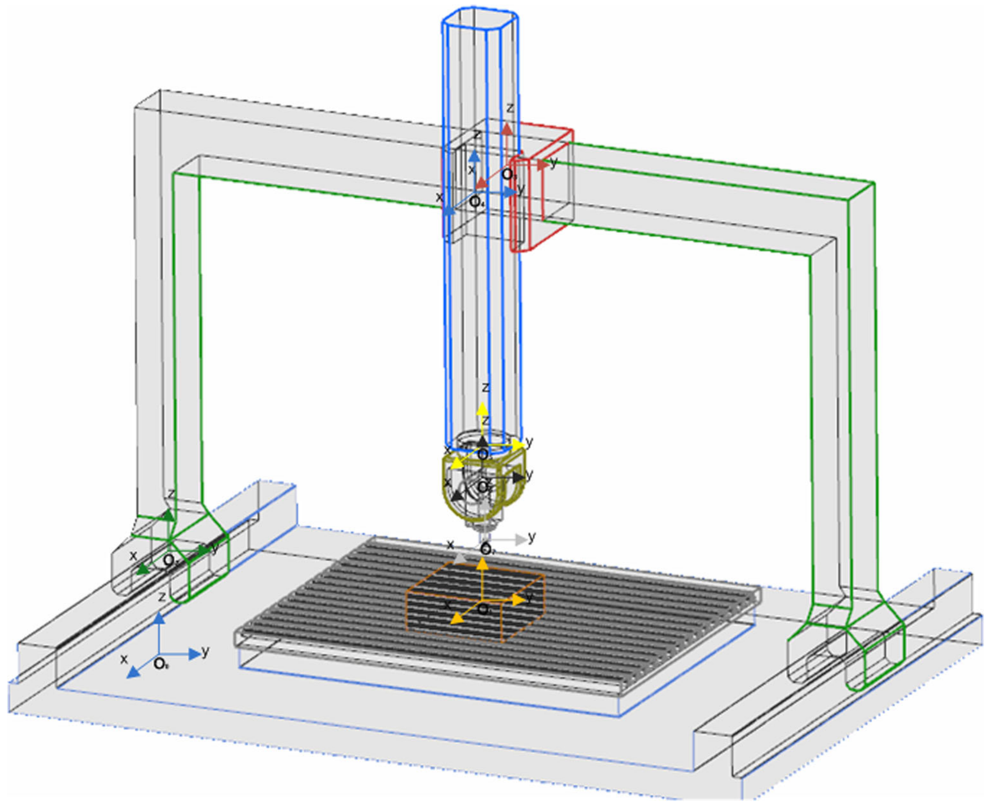

Fig. 2 The coordinate systems of every component of the machine tool

and

$$V_t = [V_{tx} \quad V_{ty} \quad V_{tz}]^T. \tag{12}$$

The cutter's posture errors (include position and orientation) *[Ex Ey Ez]* and *[Ei Ej Ek]* are then formulated as follows.

$$[E_x \quad E_y \quad E_z \quad 1]^T = {}^0_7T^7 \bullet [R_t \quad 1]^T - {}^0_1T^1 \bullet [R_w \quad 1]^T, \tag{13}$$

$$[E_i \quad E_j \quad E_k \quad 1]^T = {}^0_7T^7 \bullet [V_t \quad 1]^T - {}^0_1T^1 \bullet [V_w \quad 1]^T, \tag{14}$$

where
${}^0_7T^7 = {}^0_2T^2 * {}^2_3T^3 * {}^3_4T^4 * {}^4_5T^5 * {}^5_6T^6 * {}^6_7T^7$..
Therefore, Eqs. (13) and (14) represent the mathematical relationship between the machine tool accuracy parameters and the cutter's posture errors.

4.2 Machining profile error modeling

This section is to construct the analytical model between the cutter's posture errors and the profile errors of machined surfaces by both end milling and flank milling.

4.2.1 Profile error model of sculptured surface by end milling

End milling is an important method for sculptured surface machining. In this subsection, the mathematical relationship between the surface profile errors and the cutter's posture errors will be constructed for end milling. Normal deviation, defined as the deviation along the normal vector between the sample measurement point and its corresponding ideal point on a sculptured surface, is utilized to represent the profile error [22]. If the normal deviation at every sample point is within its tolerance, it is concluded that the machined surface satisfies the quality requirements. The mathematical relationship between these surface errors (the normal deviation) and the cutter's posture errors will be constructed below.

Figure 3 shows the surface normal errors which are affected by the cutter's posture errors at a sample point. As shown in Fig. 3(1), if there is no cutter's posture error, the cutter's contact point on the workpiece will be on the ideal surface. Because of the machine tool errors, the cutter's center point will be away from its ideal position, and therefore, there is an error associated with the center point as well as the cutter's posture as shown in Fig. 3(2). Normal and tangential errors on the surface induced by the cutter's posture errors are shown in Fig. 3(3).

As shown in Fig. 4(1), in order to describe the relationship between the cutter's posture errors and the surface errors (normal deviation), S_0 is defined as the ideal surface, and S_1 represents the actual surface after machining. P_0 is the sample point on S_0, and the actual machining point corresponding to P_0 is the point P_1 on surface S_1. The deviation between P_1 and P_0 is the error c, which is the length of the cutter's position error [*Ex*, *Ey*, *Ez*]. Point

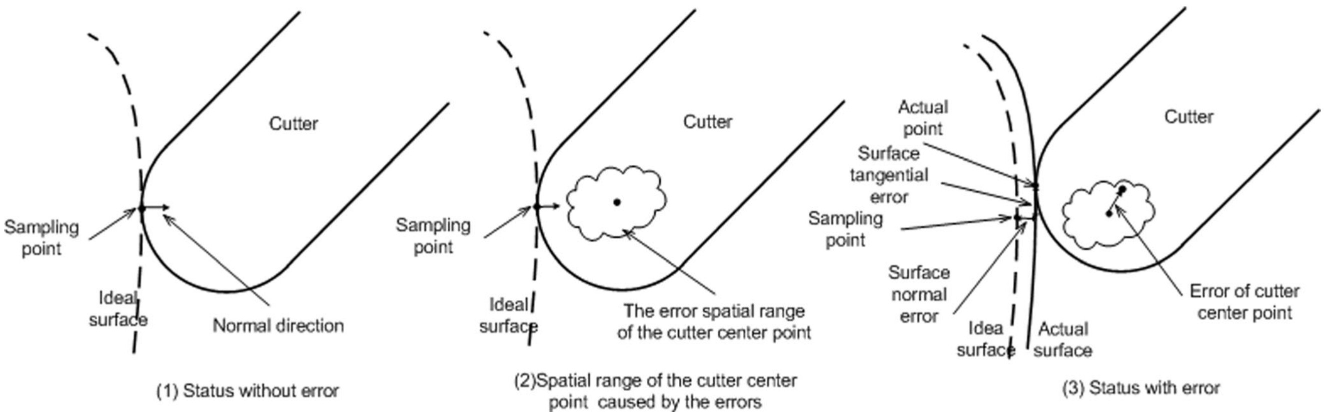

Fig. 3 Surface profile machining errors generated by cutter posture errors

P_2 on the normal direction line is the projection of P_1. The projected length of error c along the normal direction is defined as a, and the projected length along the tangential direction is defined as b. The normal of S_0 at the point P_0 intersects with S_1 at the point $P_{2'}$. The curvature radius of the surface at the sample point P_0 is represented by ρ. Because the error b and the changes of the surface normal b/ρ are very tiny, the curve $P_0P_{0'}$ can be considered as an arc curve. Then, lines $P_1P_{0'}$ and P_2P_0 are extended and intersected at points O. The line segments OP_0 and $OP_{0'}$ have an equal length of ρ.

1) First, the normal deviation at the $P_{0'}$ when cutting at P_1 is investigated. As shown in Fig. 4(2), the triangle OP_1P_2 is a right triangle; so, the deviation d can be calculated as follows.

$$d = \sqrt{(OP_0 + P_0P_2)^2 + P_1{P_2}^2} - OP_{0'} = \sqrt{(\rho + a)^2 + b^2} - \rho. \tag{15}$$

The magnitude (10^{-2}~10^{-3} mm) of error a and b is much smaller than ρ (magnitude: 10^1~10^2 mm), then,

$$d = \frac{2*a + a^2/\rho + b^2/\rho}{\sqrt{(1 + a/\rho)^2 + b^2/\rho^2} + 1} \approx \frac{2*a}{1+1} = a. \tag{16}$$

Therefore, when the cutter is at the point P_1, the normal deviation of the surface S_0 at $P_{0'}$ is a, which is the projection of error c.

2) Second, the normal deviation at the P_0 when cutting at the point of $P_{2'}$ on S_1 is investigated. As shown in Fig. 4(3), suppose P_3 is a point on the ideal surface S_0, and its corresponding point is the point $P_{2'}$ on the surface S_1. So c' is the deviation between $P_{2'}$ *and* P_3, a' and b' are the projected length of c' along the normal and tangential directions, respectively. Similar to step 1, when the cutter is at $P_{2'}$, the normal deviation of the surface S_0 at P_3 is a', which is the projection of the error c'.
3) The errors c and c' are the lengths of the cutter's position errors at point P_0 and P_3, respectively. According to Eq. (13), the directional and value differences between c and c' are ignored. So, the normal deviation at P_0 is taken as the error a, which is the projected length of the error c

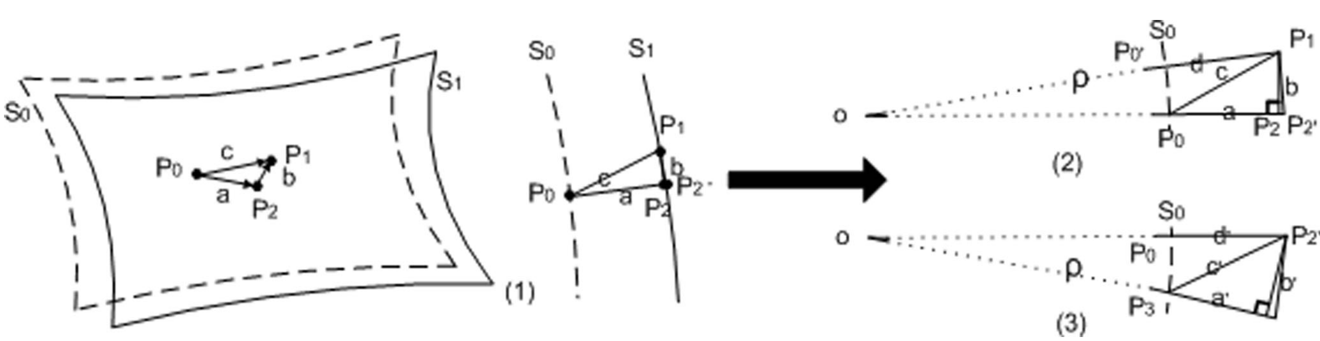

Fig. 4 Surface errors in the normal and the tangential direction

(the length of the cutter's position errors [Ex, Ey, Ez]) along the surface normal.

So, the normal deviation at a sample point is formulated as follows.

$$Nd = x_i(x_{e1}, x_{e2}, \ldots x_{e37})^* P_i + y_i(x_{e1}, x_{e2}, \ldots x_{e37})^* P_j + z_i(x_{e1}, x_{e2}, \ldots x_{e37})^* P_k \quad , \tag{17}$$

where [P_i, P_j, P_k] is the normal direction vector at the sample point, x_{e1},x_{e2}…x_{e37} the value of the machine tool accuracy parameters, and $x_i(x_{e1},x_{e2}\ldots x_{e37})$, $y_i(x_{e1},x_{e2}\ldots x_{e37})$, $z_i(x_{e1},x_{e2}\ldots x_{e37})$ are the coordinate components of the cutter's position error *[Ex, Ey, Ez]*, which is calculated by Eq. (13) at the sample point.

4.2.2 Profile error model of sculptured surface by flank milling

Flank milling is another important method for sculptured surface machining especially for ruled surface. The mathematical relationship between the surface errors (the normal deviation) and the cutter's posture errors during the flank milling will be constructed in this subsection.

The geometrical intersection element between the cutter and the surface is not a point but a short line segment as shown in Fig. 5(3). The posture errors at any point on the short line segment can be calculated by Eq. (13). The difference in calculating the cutter's position errors of these points lies only on the difference of the cutter's position transform coordinates [p_{7x} p_{7y} p_{7z}]. Assume the cutter's position transform coordinates at different points of the line segment are $[p_{7x}\ p_{7y}\ p_{7z}]_{Pi}$ *(i = 1.2.3….)*. As the line segment is very tiny (magnitude: 10^0~10^1 mm) compared to the cutter's position transform coordinates at different points $[p_{7x}\ p_{7y}\ p_{7z}]_{Pi}$ *(i = 1.2.3….)* (magnitude: 10^3 mm), the variation between the posture errors of every consecutive point on the line segment can be ignored through the calculation of Eq. (13). Then, a cutter contact point on the line segment is chosen to be analyzed to represent the points on the line segment.

Similar to the description of the end milling in Fig. 4, the error along tangential direction is ignored, and the normal deviation at P_0 is considered as the error a, which is the projection of error c, as shown in Fig. 6. So, the normal deviation at a sample point is obtained as follows, the same as Eq. (17).

$$Nd = x_i(x_{e1}, x_{e2}, \ldots x_{e37})^* P_i + y_i(x_{e1}, x_{e2}, \ldots x_{e37})^* P_j + z_i(x_{e1}, x_{e2}, \ldots x_{e37})^* P_k \quad , \tag{18}$$

where x_{e1},x_{e2}…x_{e37} are the machine tool accuracy parameters. $x_i(x_{e1},x_{e2}\ldots x_{e37})$, $y_i(x_{e1},x_{e2}\ldots x_{e37})$, $z_i(x_{e1},x_{e2}\ldots x_{e37})$ are the coordinate components of the cutter's position error *[Ex, Ey, Ez]*, which is calculated by Eq. (13) at the sample point.

5 Machine tool accuracy parameter optimization

Optimization is very important for allocating tolerances in mechanical design. After the error synthesis model between the machine tool errors and the profile errors of sculptured surfaces is constructed, the optimization constraints can be obtained by this model. An objective function based on cost-tolerance relations will be established to support the optimization process in this section.

5.1 Optimization objective construction based on a cost-tolerance function

As machine tool accuracy parameters are directly associated with the geometric tolerances of machine tool components and assemblies, cost-tolerance models [23] are adopted to construct the objective function in order to optimize these parameters.

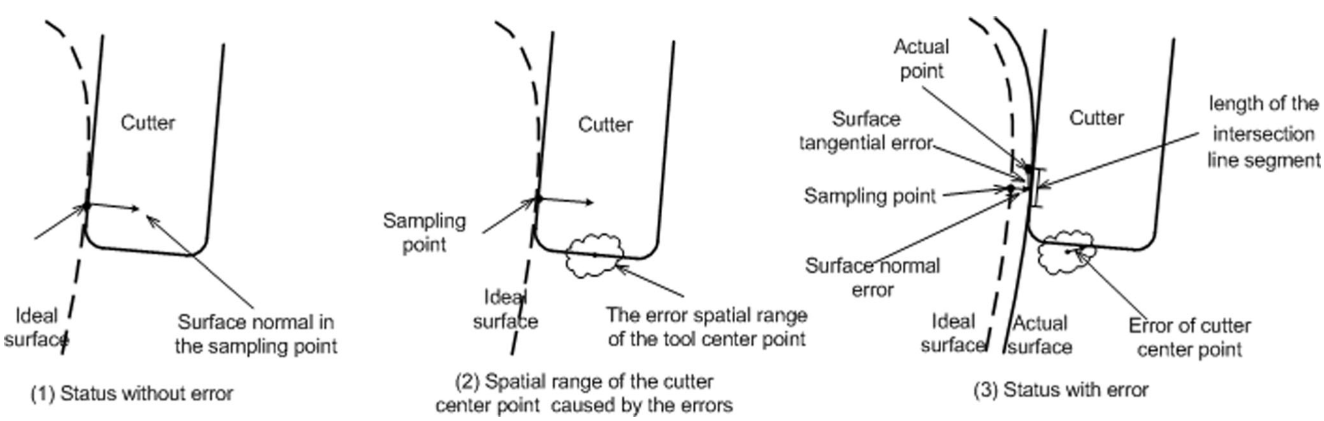

Fig. 5 Surface profile machining errors generated by cutter posture errors

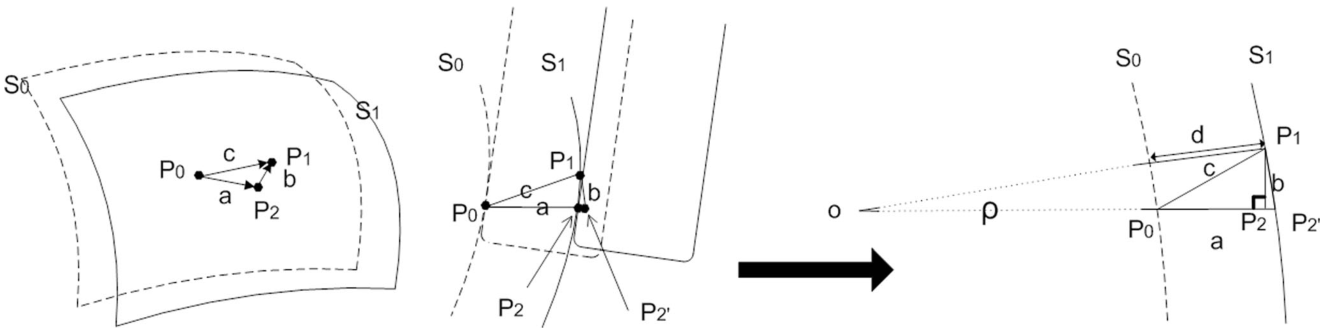

Fig. 6 Surface errors in the normal and the tangential direction

5.1.1 Cost-tolerance function

Cost-tolerance function is a common method to describe the relationship between manufacturing cost and tolerances of the mechanical products for tolerance optimization. There are several types of models for describing the cost-tolerance relationship, such as exponential model, reciprocal squared model, and reciprocal power model [23]. The machine tool accuracy parameters in this paper can be considered as the assembly tolerance. According to the description in the assembly tolerance allocation research [24], assembly cost-tolerance relationship must follow the following conditions: (a) when the tolerance $x_{\mathrm{i}} = 0$, the cost $C(x_i) = \infty$, (b) the cost $C(x_i)$ decreases with increasing tolerance x_{i}. So, the following reciprocal power model function is chosen to construct the cost-tolerance function.

$$C(x_i) = a_i + \frac{b_i}{x_i^{e_i}}, \tag{19}$$

where $C(x_i)$ is the cost of the ith parameter x_i, a_i, b_i, and e_i are the coefficients of the cost $C(x_i)$. Specially, a_i is considered as the fixed cost, and e_i the power coefficient. For errors associated with the same axis of a machine tool, as shown in Table 2, the related assembly job of these errors is completed in one operation on the axis. So, the coefficients a_i, b_i and e_i will be kept the same at this time, but they are probably different when the errors are associated with different axes of interconnected machine tool components. How to determine these coefficients is presented in Section 6.

5.1.2 Weight of the machine tool error

The weight of each machine tool error is required to reflect the error's contribution and the effect on the resultant fuzzy cost. This is very important for ensuring the validity of the optimization results. The weight coefficients of every error are formulated based on the analytic hierarchy process (AHP) method [25]. The details are presented as follows.

The machine tool errors are generated through the relative motion between the components of each kinematic pair. Suppose m represents the total number of kinematic pairs. Assembly time is taken as the measure to construct the weight coefficients, as it is a key indicator of the assembly cost. The fuzzy cost weight w_j of each kinematic pair is defined by:

$$w_j = \frac{T_j}{\sum_{k=1}^{n} T_k}, j \in \{1, 2, .., m\}, \tag{20}$$

where T_j represents the assembly time for the jth kinematic pair. The weight of each error is then considered as follows.

Suppose N represents the total number of the errors of the machine tool, and the ith error is an error belonging to the N errors of the machine tool. n_j is the number of the errors belonging to the jth kinematic pair, and the h_jth error is an error belonging to the jth kinematic pair, and it can be calculated by Eq. (21). The total number N is the sum of the $n_j(i = 1,2,\ldots m)$, as expressed in Eq. (22). Given the ith error of the entire machine tool is the h_jth error of the jth kinematic pair, Eq. (23) can be obtained.

$$n_j = \sum_{\mathrm{i}_j=1}^{n_j} h_j, \tag{21}$$

$$N = \sum_{\mathrm{j}=1}^{m} n_j, \tag{22}$$

$$i = \sum_{\mathrm{k}=1}^{j-1} n_{\mathrm{k}} + h_j. \tag{23}$$

Given the different level of difficulty in adjusting the errors of kinematic pairs during assembly, fuzzy cost weight α_{hj} of the h_jth errors of the jth kinematic pair

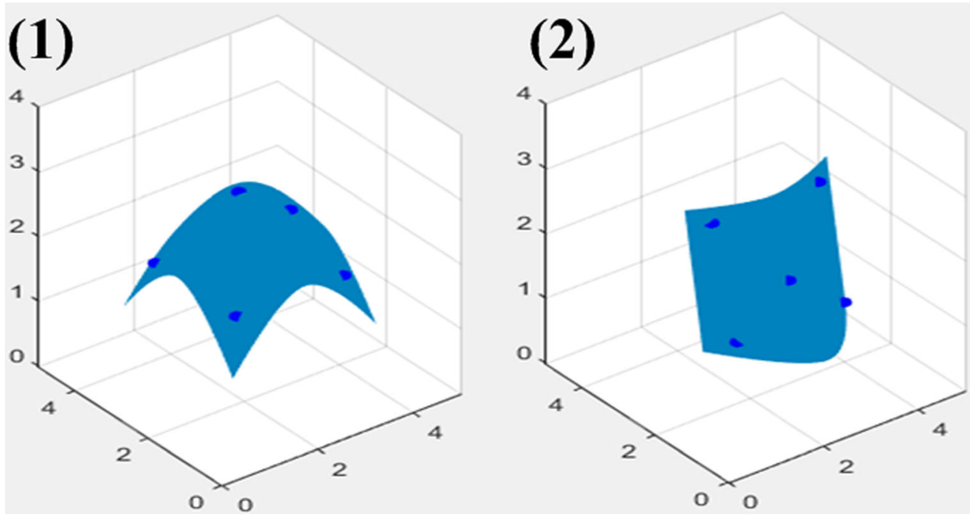

Fig. 7 The selected surface and the points. *1* End milling surface, *2* flank milling surface

is employed to represent the difficulties. So, the weight of the ith error of the entire machine tool (the h_jth error of the jth kinematic pair) is as follows:

$$w_i^f = w_{h_j}^f = \frac{\alpha_{h_j}}{\sum_{k_j=1}^{n_j} \alpha_{h_j}} * w_j, j \in \{1, 2, .., m\}. \tag{24}$$

Incorporating the cost-tolerance function obtained in Section 5.1.1, the total cost-tolerance objective function of the machine tool is defined as follows.

$$C(x) = \sum_{i=1}^{N} w_i^f * C(x_i) = \sum_{i=1}^{N} w_i^f * \left(a_i + \frac{b_i}{x_i^{e_i}} \right). \tag{25}$$

The value of the total cost $C(x)$ is to be minimized in this paper.

5.2 Optimization constraints

According to customers' requirements, the normal deviation between any two associated points of the machined and ideal surfaces should be less than the tolerance T. So, the following constraints are set.

$$abs(Nd_i) < T \quad , (i = 1, 2 ... n), \tag{26}$$

where Nd_i is the normal deviation at the ith sample points on the surface, which could be calculated by Eq. (17) and Eq. (18). The constraint is in the absolute value. In addition, a reasonable value range is assigned for each of the machine tool accuracy parameters.

$$\begin{cases} e_{1a} < x_{e1} < e_{1b} \\ e_{2a} < x_{e2} < e_{2b} \\ \quad \cdots \\ e_{37a} < x_{e37} < e_{37b} \end{cases}, \tag{27}$$

where e_{ia} and e_{ib} ($i = 1,2....,37$) are the lower and upper bounds of the ith accuracy parameter x_{ei}, respectively.

5.3 Machine tool accuracy optimization by a heuristic method

Given the constraints and the objective function, the optimization problem of this paper is a nonlinear programming problem with nonlinear constrains. As a useful heuristic, genetic algorithm is chosen for solving this multi-variable optimization problem.

6 Case study

Two surfaces, which could be machined by end milling and flank milling, respectively, are used to construct the constraints of the machine tool accuracy parameter optimization in this section. Based on the proposed methodology in this paper, the optimization result and discussion will be presented below. The optimization method is then validated through simulations.

6.1 Discussions of the optimization results

Five key points on each surface, as shown in Fig. 7, are selected to build the optimization constraints as described in Section 5.2. The machining tolerance requirement (normal

Table 3 Values of the coefficients and the optimization results

Kinematic pair belonging	Accuracy parameter X_i of the machine tool	The value of the coefficients of the objective function					Initial range(mm)		The final optimization result
		a_i	b_i	e_i	Tj	α_i	Lower bound	Upper bound	
Kinematic pair of *X*-axis	$x1$	0	0.00052816	1.1302036	6 days	1	1×10^{-3}	10×10^{-3}	4.2×10^{-3}
	$x2$	0	0.00052816	1.1302036		1	1×10^{-3}	10×10^{-3}	4.9×10^{-3}
	$x3$	0	0.00052816	1.1302036		1	1×10^{-3}	10×10^{-3}	5.8×10^{-3}
	$x4$	0	0.00052816	1.1302036		1	1×10^{-5}	5×10^{-5}	5.0×10^{-5}
	$x5$	0	0.00052816	1.1302036		1	1×10^{-5}	5×10^{-5}	5.0×10^{-5}
	$x6$	0	0.00052816	1.1302036		1	1×10^{-5}	5×10^{-5}	5.0×10^{-5}
Kinematic pair of *Y*-axis	$x7$	0	0.00220173	0.9808618	5 days	1	1×10^{-3}	10×10^{-3}	5.2×10^{-3}
	$x8$	0	0.00220173	0.9808618		1	1×10^{-3}	10×10^{-3}	6.8×10^{-3}
	$x9$	0	0.00220173	0.9808618		1	1×10^{-3}	10×10^{-3}	4.8×10^{-3}
	$x10$	0	0.00220173	0.9808618		1	1×10^{-5}	5×10^{-5}	5.0×10^{-5}
	$x11$	0	0.00220173	0.9808618		1	1×10^{-5}	5×10^{-5}	5.0×10^{-5}
	$x12$	0	0.00220173	0.9808618		1	1×10^{-5}	5×10^{-5}	5.0×10^{-5}
Kinematic pair of *Z*-axis	$x13$	0	0.00033129	1.2590875	5 days	1	1×10^{-3}	10×10^{-3}	2.9×10^{-3}
	$x14$	0	0.00033129	1.2590875		1	1×10^{-3}	10×10^{-3}	2.5×10^{-3}
	$x15$	0	0.00033129	1.2590875		1	1×10^{-3}	10×10^{-3}	3.1×10^{-3}
	$x16$	0	0.00033129	1.2590875		1	1×10^{-5}	5×10^{-5}	5.0×10^{-5}
	$x17$	0	0.00033129	1.2590875		1	1×10^{-5}	5×10^{-5}	5.0×10^{-5}
	$x18$	0	0.00033129	1.2590875		1	1×10^{-5}	5×10^{-5}	5.0×10^{-5}
Kinematic pair of *C*-axis	$x19$	0	0.00033129	1.2590875	3 days	1	1×10^{-3}	10×10^{-3}	6.8×10^{-3}
	$x20$	0	0.00033129	1.2590875		1	1×10^{-3}	10×10^{-3}	4.6×10^{-3}
	$x21$	0	0.00033129	1.2590875		1	1×10^{-3}	10×10^{-3}	1.6×10^{-3}
	$x22$	0	0.00033129	1.2590875		1	1×10^{-5}	5×10^{-5}	5.0×10^{-5}
	$x23$	0	0.00033129	1.2590875		1	1×10^{-5}	5×10^{-5}	4.8×10^{-5}
	$x24$	0	0.00033129	1.2590875		1	1×10^{-5}	5×10^{-5}	5.0×10^{-5}
Kinematic pair of *A*-axis	$x25$	0	0.00026156	1.3269297	2 days	1	1×10^{-3}	10×10^{-3}	2.6×10^{-3}
	$x26$	0	0.00026156	1.3269297		1	1×10^{-3}	10×10^{-3}	2.0×10^{-3}
	$x27$	0	0.00026156	1.3269297		1	1×10^{-3}	10×10^{-3}	4.2×10^{-3}
	$x28$	0	0.00026156	1.3269297		1	1×10^{-5}	5×10^{-5}	5.0×10^{-5}
	$x29$	0	0.00026156	1.3269297		1	1×10^{-5}	5×10^{-5}	4.8×10^{-5}
	$x30$	0	0.00026156	1.3269297		1	1×10^{-5}	5×10^{-5}	5.0×10^{-5}
Kinematic pair of X-axis	$x31$	0	0.00052816	1.1302036	6 days	1	1×10^{-5}	5×10^{-5}	5.0×10^{-5}
Kinematic pair of *Y*-axis	$x32$	0	0.00220173	0.9808618	5 days	1	1×10^{-5}	5×10^{-5}	5.0×10^{-5}
Kinematic pair of *Z*-axis	$x33$	0	0.00033129	1.2590875	5 days	1	1×10^{-5}	5×10^{-5}	4.9×10^{-5}
Kinematic pair of *C*-axis	$x34$	0	0.00033129	1.2590875	3 days	1	1×10^{-5}	5×10^{-5}	5.0×10^{-5}
	$x35$	0	0.00033129	1.2590875		1	1×10^{-5}	5×10^{-5}	5.0×10^{-5}
Kinematic pair of *A*-axis	$x36$	0	0.00026156	1.3269297	2 days	1	1×10^{-5}	5×10^{-5}	4.1×10^{-5}
	$x37$	0	0.00026156	1.3269297		1	1×10^{-5}	5×10^{-5}	5.0×10^{-5}

deviation requirement) is ±0.05 mm. The reciprocal power function is chosen as the cost-tolerance function. The cost tolerance function coefficient values of a_i, b_i, and e_i are selected from the standard data in literature [26], in which these coefficients are different when the manufacturing processes are varied or the scale of manufacturing processes are in different ranges. After consulting with machine tool manufacturers, the slideway length of *X*-, *Y*-, *Z*-, *C*-, and *A*-axes (the rolling circumferences of the rational axes are considered as the slideway lengths) is given as 3, 2, 2, 0.5, and 0.3 m,

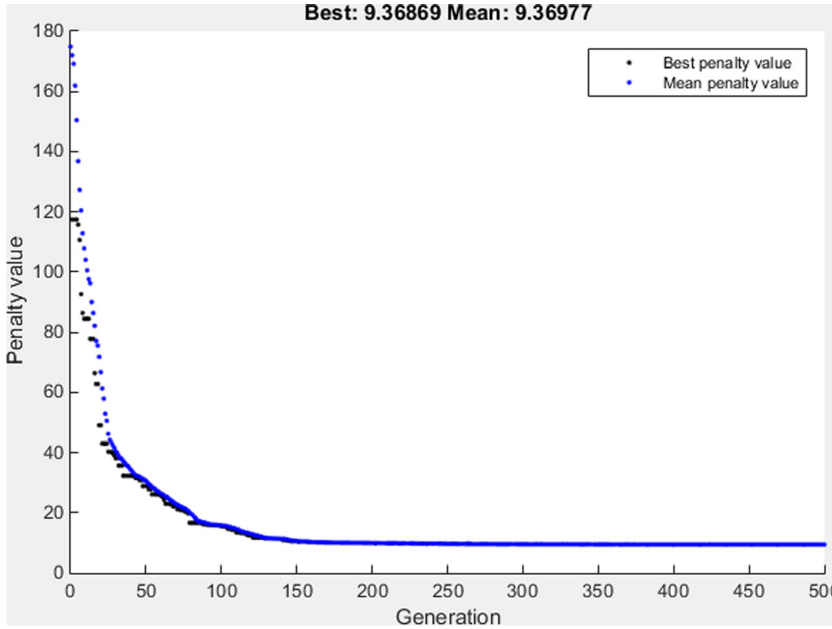

Fig. 8 Optimization process based on GA method

respectively. The lapping process of the machine tool slideway is the main job in machine tool assembly, and the slideway lengths of every axis are taken as the scale of the lapping process. According to the lapping process cost-tolerance data and the process scales, the values of a_i, b_i, and e_i are defined in Table 3. Here, the value a_i is assumed to be 0 $, because it does

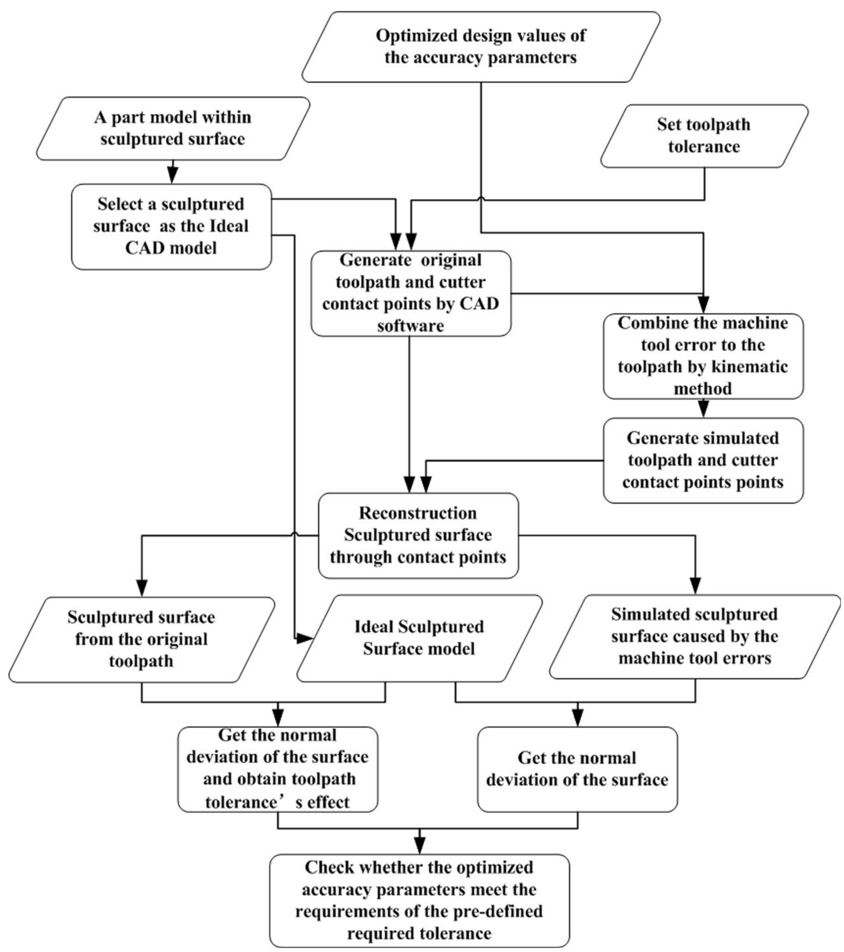

Fig. 9 Flowchart of the verification procedure

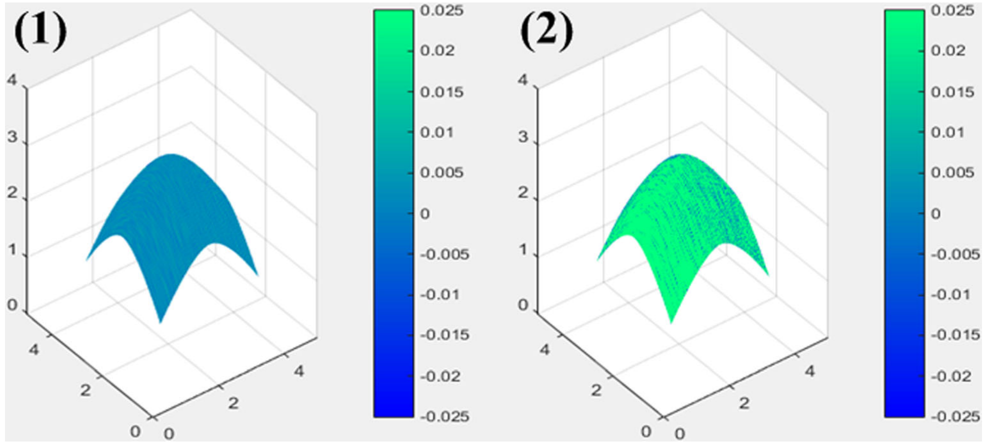

Fig. 10 The simulation of the surface of end milling. 1 Constructed by the original tool paths, *2* caused by machine tool errors

not affect the optimization calculation, while this value actually depends on the industry, since the setup cost, equipment cost, etc., will be varied from industry to industry [27]. A series of values of the assembly time T_j as described in Section 5.1.1 are given also by consultation, as shown in Table 3. The range of every machine tool accuracy parameter is determined based on the machine tool design practices. Assume the contribution of every accuracy parameter to the machine component is equal, the weight α_i is here by assumed as 1, as shown in Table 3.

The optimization results are shown in the last column of Table 3. These results are the machine tool accuracy requirements, which could then be used as a design reference of machine tool accuracy parameters. Figure 8 shows the best penalty and mean penalty fitness values during the optimization process. It can be observed that the results are an optimal solution because the penalty fitness value is decreasing when the optimization process is convergent.

6.2 Simulation verification

To check whether the above results meet the requirements of the preset tolerances, simulations of practical machining on the two surfaces are conducted using Matlab. The simulation procedure is shown in Fig. 9. First, the surfaces from the mechanical parts are exported from a CAD/CAM software (NX8.0) as the original data. The original models are shown in Fig. 7. Second, the machining tool path is generated by the CAD/CAM software for the original surface, and the tolerance of the toolpath is set as 0.005 mm, whose order of magnitude is less than accuracy of the machining tool. Third, according to the simulation manner of robots [28], the machine tool error is combined to the tool path by kinematic methods to simulate the practical machining. Then, the surfaces are reconstructed through the toolpath and the tool contact points. The two simulated surfaces constructed by the original tool paths and the tool contact points are shown in Fig. 10(1) and Fig. 11(1), respectively. The two simulated surfaces caused by machine tool errors are shown in Fig. 10(2) and Fig. 11(2), respectively. At last, by comparing the two kinds of simulated surfaces with the ideal surfaces, respectively, the normal deviation errors of the two kinds of surfaces are obtained. Then, the toolpath tolerance's effects on sculptured surfaces' machining errors are obtained, and whether the above optimized accuracy parameters results meet the requirements of the required tolerance is checked.

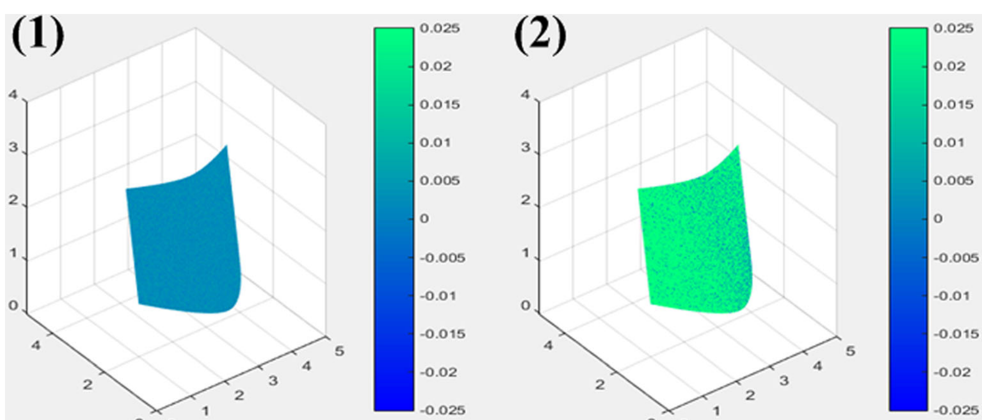

Fig. 11 The simulation of the surface of flank milling. *1* Constructed by the original tool paths, *2* caused by machine tool errors

Analysis of the surfaces is conducted using the Matlab to obtain the toolpath tolerance's effect and the machine tool errors' effect on the surfaces' machining errors. Analysis results are shown on the vertical color bar in Fig. 10 and Fig. 11. The maximum normal error is less than 0.005 mm, and it shows that the tool path computation error could be ignored in the simulation. In Fig. 10(2) and Fig. 11(2), the maximum normal error is less than 0.05 mm; so, it is concluded that the required tolerance can be achieved by using the optimized parameter values.

7 Conclusions

In this paper, a sculptured surface-oriented machining error synthesis model is proposed, as well as two new machining error generation models. The error synthesis model enables design optimization for accuracy parameters accounting customers' machining accuracy demand. An objective function is constructed based on cost-tolerance function, and an optimization algorithm based on the genetic algorithm is developed for optimizing machine tool accuracy parameters. A case study is studied, and simulation results show that both these models and the optimization approach are valid.

Acknowledgments This research was supported by National S&T Major Project Research Grant under No.2014ZX04014031.

References

1. Dornfeld D, Lee DE (2008) Precision manufacturing. Springer, New York
2. Chen GD, Liang YC, Sun YZ, Chen WQ, Wang B (2013) Volumetric error modeling and sensitivity analysis for designing a five-axis ultra-precision machine tool. Int J Adv Manuf Technol 68(9–12):2525–2534
3. Li J, Xie FG, Liu XJ (2016) Geometric error modeling and sensitivity analysis of a five-axis machine tool. Int J Adv Manuf Technol 82:2037–2051
4. Choi JP, Lee SJ, Kwon HD (2003) Roundness error prediction with a volumetric error model including spindle error motions of a machine tool. Int J Adv Manuf Technol 21(12):923–928
5. Okafor AC, Ertekin YM (2000) Derivation of machine tool error models and error compensation procedure for three axes vertical machining center using rigid body kinematics. Int J Mach Tools Manuf 40(8):1199–1213
6. Rahman M, Heikkala J, Lappalainen K (2000) Modeling, measurement and error compensation of multi-axis machine tools. Part 1: theory. Int J Mach Tools Manuf 40(10):1535–1546
7. Donaldson RR (1980) 'error budgets' in technology of machine tools. Lawrence Livermore National Laboratory, UCRL-52960-5, Berkeley
8. Krulewich DA (1998) 'a spatial-frequency-domain approach to designing precision machine tools' in thrust area report. Lawrence Livermore National Laboratory, UCRL-ID-129204, Berkeley
9. Walter M, Norlund B, Koning R, Roblee J (2014) Error budget as a design tool for ultra-precision diamond turning machines. Technical report of Precitech Inc. Access webpage: http://www.precitech.com/downloads
10. Kroll JJ (2008) 'error budgeting and certification of dimensional metrology tools' in FY07 engineering research and technology report. Lawrence Livermore National Laboratory, LLNL-TR-401927, Berkeley
11. Erkorkmaz K, Gorniak JM, Gordon DJ (2010) Precision machine tool X-Y stage utilizing a planar air bearing arrangement. CIRP Ann Manuf Technol 59(1):425–428
12. Eisenbies SK, Hocken RJ (2000) Error Budget by Constraints. ASPE Proceedings, October 22–27, Scottsdale, Arizona
13. Cheng X, Huang YM, Zhou SJ, Liu JY, Yang XH (2012) Study on the generative design method and error budget of a novel desktop multi-axis laser machine for micro tool fabrications. Int J Adv Manuf Technol 60(5–8):545–552
14. Brecher C, Utsch P, Klar R, Wenzel C (2010) Compact design for high precision machine tools. Int J Mach Tools Manuf 50(4):328–334
15. Treib T, Matthias E (1987) Error budgeting-applied to the calculation and optimization of the volumetric error field of multi-axis system. CIRP Ann Manuf Technol 36(1):365–368
16. Sun YZ, Chen WQ, Liang YC, An CH, Chen GD, Su H (2015) Dynamic error budget analysis of an ultraprecision flycutting machine tool. Int J Adv Manuf Technol 76:1215–1224
17. Ibaraki S, Sawada M, Matsubara A, Matsushita T (2010) Machining tests to identify kinematic errors on five-axis machine tools. Precis Eng 34(3):387–398
18. Callaghan R (2003) Method for establishing machine tool performance specifications from part tolerance requirements. Trans Eng Sci: Laser Metrol Mach Perform VI 44:507–516
19. Ramesh R, Mannan MA, Poo AN (2000) Error compensation in machine tools-a review part I: geometric, cutting-force induced and fixture dependent errors. Int J Mach Tools Manuf 40(9):1235–1256
20. Bohez ELJ (2002) Five-axis milling machine tool kinematic chain design and analysis. Int J Mach Tools Manuf 42(4):505–520
21. Tian WJ, Gao WG, Zhang DW, Huang T (2014) A general approach for error modeling of machine tools. Int J Mach Tools Manuf 4(79):17–23
22. Helmel Engineering Products Inc (2011) Curved surface measurement with vector point. Technical Note, January 15
23. Chase KW (1999). Minimum-cost tolerance allocation. Research Report of ADCATS (Association for the Development of Computer-Aided Tolerancing Systems), No. 99–5
24. Lin CY, Huang WH, Jeng MC, Doong JL (1997) Study of an assembly tolerance allocation model based on Monte Carlo simulation. J Mater Process Tech 70(1–3):9–16
25. Ayag Z, Ozdemir RG (2006) A fuzzy AHP approach to evaluating machine tool alternatives. J Intell Manuf 17(2):179–190
26. Chase KW (1999) Tolerance allocation methods for designers. Research Report of ADCATS (Association for the Development of Computer-Aided Tolerancing Systems), No 99–6
27. Prabhaharan G, Asokan P, Ramesh P, Rajendran S (2004) Genetic-algorithm-based optimal tolerance allocation using a least-cost model. Int J Adv Manuf Technol 24(9):647–660
28. Rout BK, Mittal RK (2006) Tolerance design of robot parameters using Taguchi method. Mech Syst Signal Pr 20(8):1832–1852